Effective Medium Theory for the Elastic Properties of Composites and Acoustics Applications

MITRE

Effective Medium Theory for the Elastic Properties of Composites and Acoustics Applications

P. J. Steinhardt

February 1992

JSR-91-112

JASON
The MITRE Corporation
7525 Colshire Drive
McLean, Virginia 22102-3481
(703) 883-6997

REPORT DOCUMENTATION PAGE

Form Approved
OMB No. 0704-0188

1. AGENCY USE ONLY (Leave blank)	2. REPORT DATE	3. REPORT TYPE AND DATES COVERED
	March 3, 1992	Final

4. TITLE AND SUBTITLE

Effective Medium Theory for the Elastic Properties of Composites and Acoustics Applications

5. FUNDING NUMBERS

PR - 8503Z

6. AUTHOR(S)

P. J. Steinhardt

7. PERFORMING ORGANIZATION NAME(S) AND ADDRESS(ES)

The MITRE Corporation
JASON Program Office A020
7525 Colshire Drive
McLean, VA 22102

8. PERFORMING ORGANIZATION REPORT NUMBER

JSR-91-112

9. SPONSORING / MONITORING AGENCY NAME(S) AND ADDRESS(ES)

DARPA/TIO
3701 North Fairfax Drive
Arlington, Virginia 22203-1714

10. SPONSORING / MONITORING AGENCY REPORT NUMBER

JSR-91-112

11. SUPPLEMENTARY NOTES

12a. DISTRIBUTION / AVAILABILITY STATEMENT

Approved for public release. Distribution Unlimited

12b. DISTRIBUTION CODE

13. ABSTRACT *(Maximum 200 words)*

We derive an effective medium theory that predicts the bulk and shear moduli of composite materials consisting of a matrix material with soft or hard ellipsoidal inclusions. The theory predicts that disk-shaped inclusions are most effective for softening or hardening a composite material. The theory is applied to the design of materials with highly absorptive acoustical properties.

14. SUBJECT TERMS

medium theory for elastic properties, inclusion shape, theory for dielectrics, acoustic reflection,

15. NUMBER OF PAGES

41

16. PRICE CODE

17. SECURITY CLASSIFICATION OF REPORT	18. SECURITY CLASSIFICATION OF THIS PAGE	19. SECURITY CLASSIFICATION OF ABSTRACT	20. LIMITATION OF ABSTRACT
UNCLASSIFIED	UNCLASSIFIED	UNCLASSIFIED	SAR

Abstract

We derive an effective medium theory that predicts the bulk and shear moduli of composite materials consisting of a matrix material with soft or hard ellipsoidal inclusions. The theory predicts that disk-shaped inclusions are most effective for softening or hardening a composite material. The theory is applied to the design of materials with highly absorptive acoustical properties.

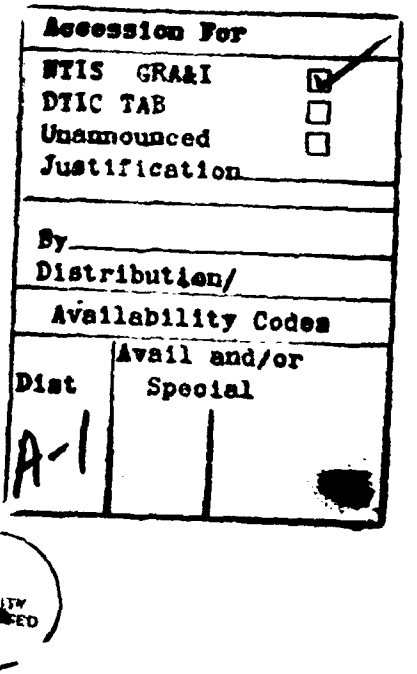

Contents

1 INTRODUCTION

The effect of impurities or inclusions on the elastic properties of otherwise homogeneous materials is important in understanding the behavior of natural (e.g., geological) materials and in developing synthetic composites for applications. Theoretical analyses have been developed to explain the elastic behavior of porous rocks (*Korringa, et al.*, 1979), to predict the strengthening effect of thin fibers in composites (*Hill*, 1963), and to describe the properties of polycrystalline materials (*Zeller and Dederichs*, 1973).

An exact calculation of the elastic properties is not possible unless the precise distribution of the inclusions is given. Specialized placement of inclusions, especially voids, can have major effects. However, for most purposes, the inclusions can be treated statistically. Various approximation schemes have been developed assuming a random distribution of inclusions. Einstein (*Einstein*, 1906) considered the effect of a low concentration of spherical inclusions. Beginning with Wu (*Wu*, 1966), a number of different approaches were developed to extend the analysis to ellipsoidal inclusions and to relatively higher densities. Wu's approach is a static derivation which treats the composite as an effective medium for which modified or "effective" elastic constants can be computed self-consistently. A second, dynamical approach evaluates the diffraction of sound waves from a random distribution of ellipsoidal inclusions in the limit of zero frequency (*Berryman*, 1980) to determine the effective bulk and shear moduli. A third approach is to derive rigorous bounds on the effective elastic constants based on variational principles ap-

plied to the strain energy (*Hashin and Shtrikman*, 1962). A review can by found in *Watt, Davies, and O'Connell*, 1976.

In this paper, we derive a self-consistent effective medium theory for ellipsoidal inclusions that is closely related to Wu's. It is equally valid but somewhat simpler than Wu's in the limit of low concentration of inclusions, which will be the case of interest here. The theory is used to show how the softening (or hardening) of a material is effected by shape. In particular, we find that, for the same fractional volume, disk-shaped voids or cracks are significantly more effective in softening than needle-shaped or spherical voids. As the aspect ratio of the disks or cracks approaches zero, an infinitessimal concentration is sufficient to dramatically soften the material; the same is not true for needle-shaped or spherical voids.

The results from the effective medium theory are used to suggest the design of acoustic absorbing composite materials. This work is motivated by an earlier JASON study of composite dielectric materials that may reduce light reflectivity (*Nelson*, 1990). Although many of the principles are similar, we find interesting and important differences between the acoustical and electromagnetic problem which suggest that thin accoustic absorption coatings are more difficult to achieve than thin electromagnetic absorption coatings.

The plan of the paper is as follows: In Section 2, we derive the effective medium theory for a homogeneous matrix with ellipsoidal inclusions. The effective bulk and shear moduli of the composite are computed in terms of the elastic constants of the matrix and inclusions and the aspect ratio of

the inclusions. We analyze the results of the effective medium theory to determine how the shape of the voided inclusions can dramatically effect the degree to which they soften a material. In Section 3, we consider the reflection of sound waves propagating in a liquid medium at the interface between the liquid and the composite material. Based on the effective medium theory, we discuss the conditions for composite material optimal for acoustic absorption.

2 EFFECTIVE MEDIUM THEORY FOR THE ELASTIC PROPERTIES OF COMPOSITE MATERIALS

In this section, we will develop an effective medium theory to determine the effective bulk and shear moduli for a composite medium with a random spatial and orientational distribution of identical ellipsoidal inclusions. The composite can be treated as an effective medium for excitation frequencies whose wavelength is large compared to the size of the inclusions.

2.1 The Strain Field in the Effective Medium

Consider a composite material under compression, $d(x)$, and/or shear, $s_{ij}(x)$; that is, the strain is

$$\epsilon_{ii} = d(x)$$

$$\epsilon_{ij}(x) = s_{ij}(x) + \frac{1}{3}d(x)\delta_{ij}$$

where the usual summation convention for repeated indices is adopted. The stress tensor is given by

$$\sigma_{ij} = (K - \frac{2}{3}G)\epsilon_{kk}\delta_{ij} + 2G\epsilon_{ij},$$

where K and G are the bulk and shear moduli, respectively. For the composite material, K and G are spatially varying; we will treat $K(x)$ and $G(x)$ as step functions assuming values K_m and G_m in the matrix and values K_i and G_i in the inclusions. We want to determine the effective bulk and shear

moduli, K_* and G_*, in terms of K_m, G_m, K_i, G_i, the fractional volume occupied by the inclusions, f, and the aspect ratio of the ellipsoidal inclusions, α.

In the effective medium approximation, we have

$$\begin{aligned} < K(x)\, d(x) > &= K_* < d(x) > \\ < G(x)\, s(x) > &= G_* < s(x) > \end{aligned} \qquad (2-1)$$

(where we have dropped tensor subscripts); consequently,

$$\begin{aligned} (1-f)(K_m - K_*) < d(x) >_m + f(K_i - K_*) < d(x) >_i &= 0 \\ (1-f)(G_m - G_*) < s(x) >_m + f(G_i - G_*) < s(x) >_i &= 0; \end{aligned} \qquad (2-2)$$

$<>_m$ and $<>_i$ represent the averages over all matrix and inclusion regions, respectively, which can be related to the average over the composite:

$$\begin{aligned} < d(x) >_{i\,(m)} &= t_{i\,(m)} < d(x) > \\ < s(x) >_{i\,(m)} &= v_{i\,(m)} < s(x) > . \end{aligned} \qquad (2-3)$$

Here we have used the average spatial and orientational isotropy of the medium to express the relations in terms of scalar strain factors, t and v. Equation (2-1) can then be re-expressed as:

$$\begin{aligned} K_* &= \frac{(1-f)K_m t_m + f K_i t_i}{(1-f)t_m + f t_i} \\ G_* &= \frac{(1-f)G_m v_m + f G_i v_i}{(1-f)v_m + f v_i} \end{aligned} \qquad (2-4)$$

2.2 Calculation of Strain Factors, t and v

For our effective medium theory, we assume a low fractional volume of inclusions, $f \ll 1$, in which case $t_m \approx 1$ and $v_m \approx 1$. The technical part of the computation is to determine the strain factors, t_i and v_i. For this, we

first consider the strain field, ϵ_{ij} in a single inclusion imbedded in the matrix material. Eshelby (*Eshelby*, 1957) has shown that the strain in the ellipsoid satisfies:

$$\epsilon_{ij} = \epsilon^0_{ij} + \int d^3x' G_{ijkl}(x - x')\Delta c_{klmn}(x')\epsilon_{mn} \qquad (2-5)$$

where ϵ^0_{ij} is the strain field for a completely homogenous medium under the same stress conditions, $G_{ijkl}(x-x')$ is the homogeneous green's function, and

$$\Delta c_{ijkl}(x) \equiv [K(x) - K_m - \frac{2}{3}(G(x) - G_m)]\delta_{ij}\delta_{kl} + [G(x) - G_m](\delta_{ik}\delta_{jl} + \delta_{il}\delta_{jk}).$$

The homogeneous green's function is

$$G_{ijkl}(x - x') = \frac{1}{4}(\partial_j\partial_l g_{ik} + \partial_i\partial_l g_{jk} + \partial_j\partial_k g_{il} + \partial_i\partial_k g_{jl}), \qquad (2-6)$$

where $g_{ij}(x - x')$ is the displacement at point x caused by a unit force in the jth direction at point x' in the homogeneous medium:

$$g_{ij}(x) = \frac{1}{32\pi G_m(1+y)}\left[(5-4y)\frac{\delta_{ij}}{|x-x'|} + (1+4y)\frac{x_i x_j}{|x-x'|^3}\right], \qquad (2-7)$$

and

$$y \equiv \frac{3K_m}{4G_m}. \qquad (2-8)$$

In our approximation of treating $K(x)$ and $G(x)$ as a step-function, $\Delta c_{ijkl}(x)$ is only non-zero within the inclusions. Eshelby has also shown that the strain is spatially uniform within the ellipsoidal inclusion. Hence, the solution to the integral equation can be written:

$$\epsilon_{ij} = T_{ijkl}\epsilon^0_{kl} \qquad (2-9)$$

where T_{ijkl} is a constant tensor. If we write

$$\int d^3x' G_{ijkl}(x - x')\Delta c_{klmn}(x')\epsilon_{mn} = -A_{ijkl}\,\Delta c_{klmn}\epsilon_{mn},$$

then the T_{ijkl} in Equation (2-9) can be written:

$$T = [I + A\ \Delta c]^{-1}. \qquad (2-10)$$

The tensor A, the integral of $-G$ over the volume of the ellipsoid, is the source of the shape dependent contributions. The only non-zero elements of A are A_{ijij} and A_{iijj}, including A_{iiii}, which are straightforward although tedious to compute. There remains the even more tedious task of inverting $I + A\ \Delta c$ to obtain T, and then averaging over the orientations of the ellipsoid. The average T is an isotropic tensor:

$$\bar{T}_{ijkl} = \frac{1}{3}(t_i - v_i)\delta_{ij}\delta_{kl} + \frac{1}{2}v_i(\delta_{ik}\delta_{jl} + \delta_{il}\delta_{jk}), \qquad (2-11)$$

from which one can read off the desired strain factors, t_i and v_i. A simplification is that one can avoid the explicit average over orientations by employing a theorem due to Kroner (*Kroner*, 1958), which states that

$$\begin{aligned} t_i &= \tfrac{1}{3}T_{iikk} \\ v_i &= \tfrac{1}{5}(T_{ikik} - \tfrac{1}{3}T_{iikk}), \end{aligned} \qquad (2-12)$$

where the tensors on the right-hand side are before orientational averaging.

With the aid of Mathematica$_{\mathrm{TM}}$, we have computed the strain factors t_i and v_i by this method. For an ellipsoid with axes $a_3 = \alpha a_1 = \alpha a_2$ (α is the "aspect ratio" for the inclusions and a_1 and a_2 are held fixed), we obtain

$$\begin{aligned} t_i &= \{\tfrac{1-k}{1+y} + k \\ &\quad -y\tfrac{(1-k)(1-g)}{(1+y)^2}J^2(1-\alpha^2)^2\left[g + \tfrac{1-g}{4(1+y)}\ (1 - (3 + (4y+2)(1+2\alpha^2))J)\right]^{-1}\}^{-1}, \\ v_i &= \tfrac{1}{5}\{\frac{\frac{1-k}{1+y}+k}{g+\frac{1-g}{1+y}(\frac{1}{4}-\frac{3}{4}J+(y+\frac{1}{2})(1+2\alpha^2)J)}t_i \\ &\quad + \left[(\tfrac{1}{4}(y+\tfrac{3}{4}) + (\tfrac{1}{4}y + \tfrac{5}{16} - \tfrac{1}{4}\alpha^2)J)\tfrac{1-g}{1+y} + \tfrac{1}{2}g\right]^{-1} \\ &\quad + \left[\tfrac{1-g}{2(1+y)}(y + \tfrac{1}{2} - (y + \tfrac{1}{2} + y\alpha^2)J) + \tfrac{1}{2}g\right]^{-1}\}, \end{aligned} \qquad (2-13)$$

where

$$g \equiv \frac{G_i}{G_m},$$

$$k \equiv \frac{K_i}{K_m},$$

$$J = \frac{1}{1-\alpha^2} + \frac{3\alpha}{2(1-\alpha^2)^2}\left[\alpha - \frac{\cos^{-1}\alpha}{(1-\alpha^2)^{\frac{1}{2}}}\right]$$

and

$$y \equiv \frac{3K_m}{4G_m}.$$

From the strain factors computed in the previous subsection, the effective bulk and shear moduli can be determined from Equation (2-4). Note that the assumption of a small density of inclusions affects the computation in two ways. First, we assume that $t_m \approx 1$; that is, the average strain in the matrix is nearly identical to what it would have been if the medium were homogeneous. Second, the computation of t_i relied on the strain field for a single inclusion imbedded in a matrix whose elastic constants we took to be K_m and G_m; consequently, Equation (2-4) is an explicit expression for K_* and G_* in terms of the elastic constants of the homogeneous materials. By contrast, Wu (*Wu*, 1963) and others take the external elastic constants to be K_* and G_*. Equation (2-4) is then an implicit, self-consistent equation which can be solved for K_* and G_*. The two approaches agree in the limit of small inclusion concentration ($f \ll 1$), the limit of interest for this paper, but our explicit expression is simpler to analyze. Neither approach is valid in the limit of very high inclusion concentration since inclusion interactions are ignored in either case.

2.3 Dependence of Effective Elastic Constants on Inclusion Shape

The general expressions for the effective elastic constants obtained by combining Equations (2-4) and (2-13) are complex, but the basic behavior can be appreciated by taking the limit of inclusions that are soft (compared with the matrix material), $K_i \ll K_m$ and $G_i \ll G_m$. We will use the results to show that thin-disk inclusions are the most effective in altering the elastic constants of composite materials.

For a spherical inclusion ($\alpha = 1$ and $J = 1/5$), the strain factors are:

$$\begin{aligned} t_{(S)} &= \frac{y+1}{ky+1} \\ v_{(S)} &= \frac{5y+5}{g(2y+3)+3y+2} \end{aligned} \qquad (2-14)$$

where g and y are as defined below Equation (2-13) at the end of the previous subsection. In the limit of a disk-like inclusion ($\alpha \ll 1$), the strain factors are:

$$\begin{aligned} t_{(D)} &= \frac{4y+4}{\frac{3K_i+4G_i}{G_m}+\frac{3\pi\alpha(y+\frac{1}{2})}{y+1}} \\ v_{(D)} &= \frac{2}{5}\Big[1+\frac{y+1}{g+\frac{3\pi\alpha}{8}(2y+1)} \\ &\quad +\frac{1+3K_i/G_m}{2(y+g)}t_{(D)}\Big]. \end{aligned} \qquad (2-15)$$

In the limit of needle-shaped inclusions ($\alpha \gg 1$), the strain factors are:

$$\begin{aligned} t_{(N)} &= \frac{(1+y)(3+4y)}{3+3y+2ky+2ky^2} \\ v_{(N)} &= \frac{1}{5}\Big[\frac{4}{1+g}+\frac{16(1+y)}{1+4y+g(3+4y)}+\frac{4(1+ky)}{3+4y+4g}t_{(N)}\Big] \end{aligned} \qquad (2-16)$$

Note that the strain factors for needle-like and sphere-like inclusions approach non-zero constant values in the limit of soft inclusions (e.g., inclusions

filled with air), $K_i \to 0$ and $G_i \to 0$ or, equivalently, $k \to 0$ and $g \to 0$. By Equation (2-4), K_* and G_* only approach K_i and G_i, respectively, as $f \to 1$. That is, the composite soften's only if the fractional volume of soft inclusions is nearly unity.

For the disk-like inclusions, $t_{(D)}$ and $v_{(D)}$ are proportional to $1/\alpha$ in the limit $k \to 0$ and $g \to 0$; consequently, even if the fractional volume occupied by the inclusions is very small, their effect on the elastic constants of the composite can be very big in the limit of thin-disks $\alpha \to 0$ (e.g., cracks). As the disks become thinner, the strain factors $t_{(D)}$ amd $v_{(D)}$ diverge and Equation (2-4) implies

$$\begin{aligned} K_* &\approx \frac{K_m}{1+ft_{(D)}} \propto \alpha K_m \\ G_* &\approx \frac{G_m}{1+fv_{(D)}} \propto \alpha G_m \end{aligned} \qquad (2-17)$$

(recall $K_i = G_i = 0$).

One might also consider inclusions with small G_i but non-negligible K_i (e.g., inclusions of liquid). In this case, $v_{(D)}$ diverges and $G_* \propto \alpha G_m$; however, K_* is not significantly altered.

To properly understand these conclusions, some attention has to be given as to the order of limits. Consider now the case of non-zero but small K_i and G_i in Equation (2-15). We wish to consider the limit where the α-dependent contribution to the denominator of $t_{(D)}$ and to the denominator of the second and third terms of $v_{(D)}$ dominates over the K_i- or G_i-dependent terms, and yet remain small compared to unity. Hence, the more precise statement of our conclusion is as follows: The shear modulus diverges in the limit that G_i, $\alpha \to 0$ provided $\alpha > (8/3\pi)G_i/G_m$; the bulk modulus diverges

in the limit $\alpha,\ K_i,\ G_i \to 0$ provided $\alpha > (4\pi/3)(3K_i + 4G_i)/G_m$.

Figure 2-1 shows the predicted strain factors, $t_{(D)}$ and $v_{(D)}$, for thin-disks as a function of the aspect ratio, α, where we have taken $K_i = G_i = 0$ with $K_m = G_m = 1$. In Figure 2-2, we show the effective medium predictions for the bulk modulus as a function of fractional volume of inclusions, f, for (a) disk-like ($\alpha = 0.001$), (b) sphere-like ($\alpha = 1$), and (c) needle-like ($\alpha = 1000.$) inclusions. In all three cases, the bulk modulus approaches zero (or, more generally, the bulk modulus of the inclusion, k_i) in the limit that $f \to 1$. However, a tiny fraction of disk-like inclusions is sufficient to dramatically soften the composite. (The same effective medium expressions can be used to show that hard disks are most effective in hardening materials, as well, although the difference is less dramatic. In real applications, hard disks have the disadvantage that, while they may effectively increase the bulk modulus, they also increase the susceptibility to cracking; hence, needle-like fibers rather than disk-like inclusions are introduced for hardening purposes.) Figure 2-3 shows how the bulk, shear and Young's moduli, $E = [9KG/(3K + G)]$, change with aspect ratio in the limit of disk-like inclusions ($\alpha \ll 1$).

2.4 Comparison with Effective Medium Theory for Dielectrics

The effective medium theory for the elastic behavior of composites developed here is motivated by a similar effective medium theory for describing the dielectric behavior of composites. For the dielectric problem, one con-

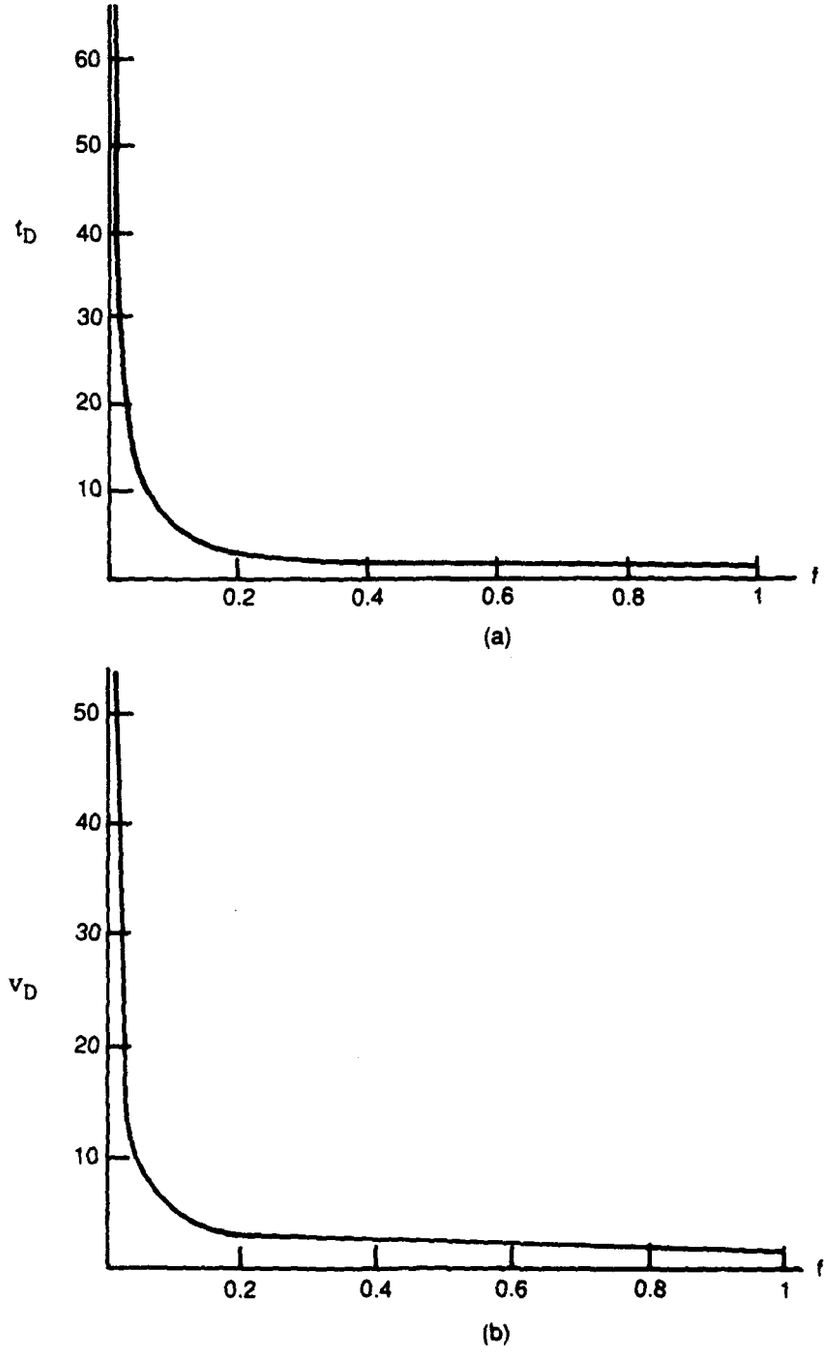

Figure 2-1. Bulk (t_D) and shear (v_D) strain factors as a function of aspect ration, d, for disk-like inclusions with $K_i = G_i = 0$.

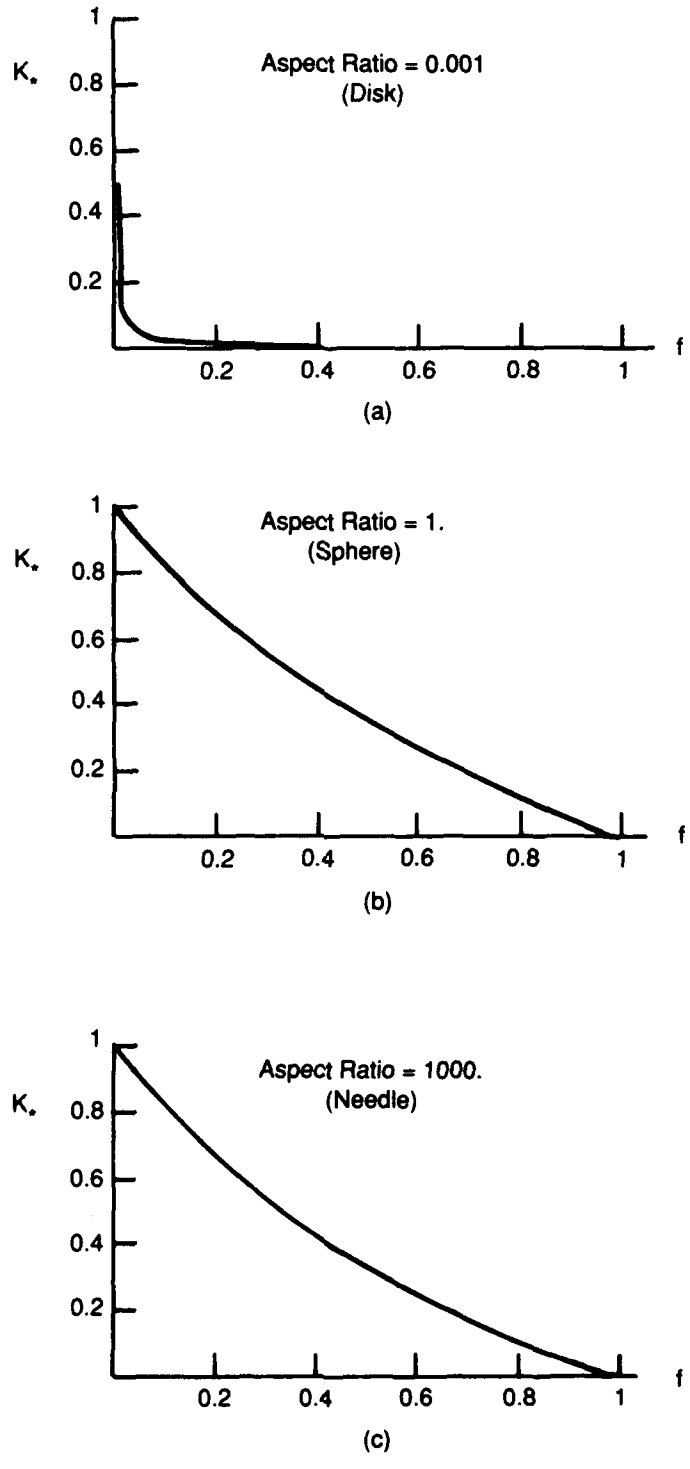

Figure 2-2. Effective bulk modulus, K*, as a function of fractional inclusion volume, f, for disk-like, sphere-like, and needle-like inclusions.

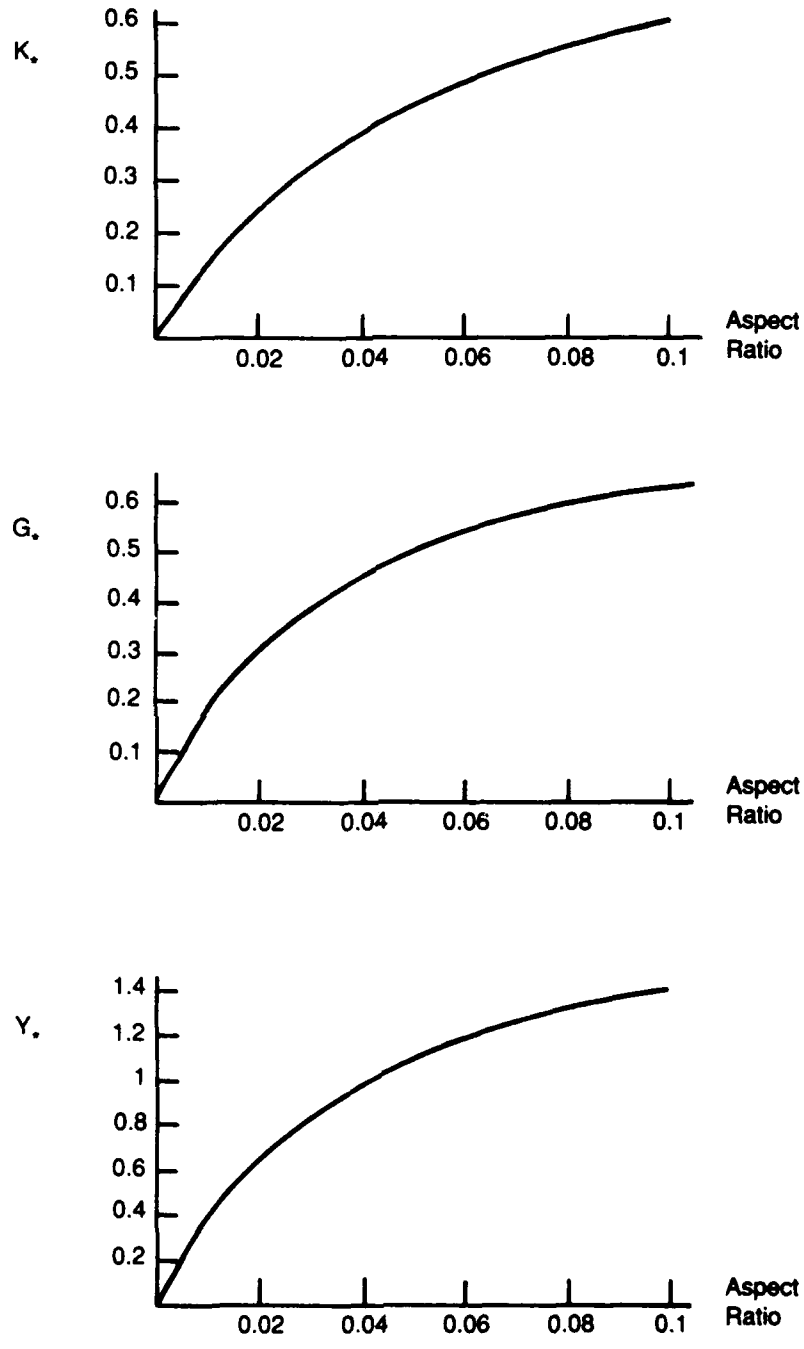

Figure 2-3. Effective bulk (K_*), shear (G_*) and Young's modulus for disk-like inclusions as a function of aspect ratio (fractional volume f = .1).

siders a matrix with dielectric constant ϵ_m with ellipsoidal inclusions with dielectric constant ϵ_i; an effective medium approximation is used to determine an effective dielectric constant ϵ_* as a function of the dielectric constants of the component materials and the fractional volume and aspect ratio of the inclusions. It is instructive to consider some of the similarities and differences between the two effective medium theories.

The effective medium theory for elasticity developed here is analogous to the Maxwell-Garnett (*Maxwell-Garnett*, 1904) effective medium approximation for dielectrics. In the Maxwell-Garnett theory, one begins by considering the electric field for a single ellipsoidal inclusion in an otherwise homogeneous matrix. A key simplification is that the electric field is spatially uniform within the ellipsoidal inclusion; this is analogous to Eshelby's result used in the elasticity argument that the strain field is spatially uniform within an ellipsoidal inclusion. The electric field inside the inclusion is related to the average electric field in the composite by

$$\mathbf{E}_i = t_i \, \mathbf{E}_*.$$

Here the factor t_i plays the same role as the strain factor t_i in the elasticity theory. In principle, a similar relation can be written to relate the electric field in the matrix to the average field in the composite (leading to a second factor, t_m). However, in the Maxwell-Garnett approximation, a small fractional volume of inclusions is assumed such that $t_m \approx 1$. Also, t_i is computed in terms of the dielectric constant in the inclusion and the dielectric constant in the composite; in the limit of small fractional volume of inclusions, the dielectric constant of the matrix is substituted for the dielectric constant of the composite. These approximations are completely analogous

to the approximations in the effective medium theory discussed here.

As a function of aspect ratio, we have found that the most dramatic effect on the elastic behavior of solids occurs in the limit of soft ($K_i \approx 0$, $G_i \approx 0$) *disk-like* inclusions. A similar dramatic effect occurs for dielectrics occurs in the limit of conducting ($\epsilon_i \rightarrow \infty$) *needle-like* inclusions. The effective dielectric constant of the medium diverges for any finite fractional volume of conducting inclusions as the aspect ratio of the conducting inclusions increases. An expression similar to Equation (2-4) can be derived, except with the elastic constant replaced by the dielectric constant.

Although there are these similarities in the dielectric and elastic problems, some differences arise as well. First, the dielectric constant diverges in the limit of conducting inclusions, whereas the elastic constants approach zero in the limit of soft inclusions. Also, one finds that $t_i \rightarrow 0$ in the limit of conducting needles, whereas we found t_i diverges in the limit of soft disks. Consequently, the behavior of Equation (2-4) is different in the dielectric analogue. Whereas the denominator on the right-hand-side diverges for the elastic case (forcing the elastic constants to soften), the denominator is irrelevant and the numerator diverges in the dielectric problem (forcing the dielectric constant to diverge).

Beyond these technical differences, there is the qualtitative difference in the dependence on aspect ratio, which can be understood intuitively in terms of the difference between the vector-like electric field versus tensor-like stress field. For the dielectric problem, the dielectric constant is large in a medium in which it is "easy" to separate charge. Thin conducting nee-

dles can separate charge most effectively as a function of their volume. In particular, a single thin needle stretching across the entire composite (from contact to contact) forms a conducting bridge that makes the effective dielectric constant diverge. Presumably, a conducting thin disk would have the same effect. By contrast, a needle-like air or void inclusion in a solid does not dramatically alter the elastic properties far from the inclusion; instead, a planar or disk-like layer is more effective. In particular, a single disk stretching across the composite forms a soft layer that causes the elastic constant of the composite to dramatically shrink. The results of our technical analysis seem more plausible in light of these remarks.

3 APPLICATION OF COMPOSITES FOR ACOUSTIC ABSORPTION

In this Section, we show how the effective medium theory for the elastic behavior of composites can be used to suggest the design of composite materials that reduce acoustic reflection. We consider the reflection of plane sounds waves from a liquid medium (which we will take to be water) impinging on a planar surface of a semi-infinite composite material. The calculation is relevant for wavelengths short compared to the dimensions of the composite slab but long compared to the size of the inclusions.

3.1 Reflection Coefficient for Scattering at a Liquid-Solid Interface

The geometry is shown in Figure 3-1. The incident and reflected sound waves in the liquid (water) are longitudinal waves. (We assume the reflected transverse wave in the water is negligible.) The angle of incidence is equal to the angle of reflection. Both longitudinal and transverse refracted waves are generated in the composite. The angles for propagation of the refracted waves satisfy

$$\frac{\sin\theta}{\sin\theta_{l,t}} = \frac{c_W}{c_{l,t}}, \qquad (3-1)$$

where c_W is the speed of sound, θ is the angle of incidence, $\theta_{l,t}$ is the refraction wave of the longitudinal and transverse wave, respectively, and $c_{l,t}$ is the effective longitudinal and transverse sound speed in the composite.

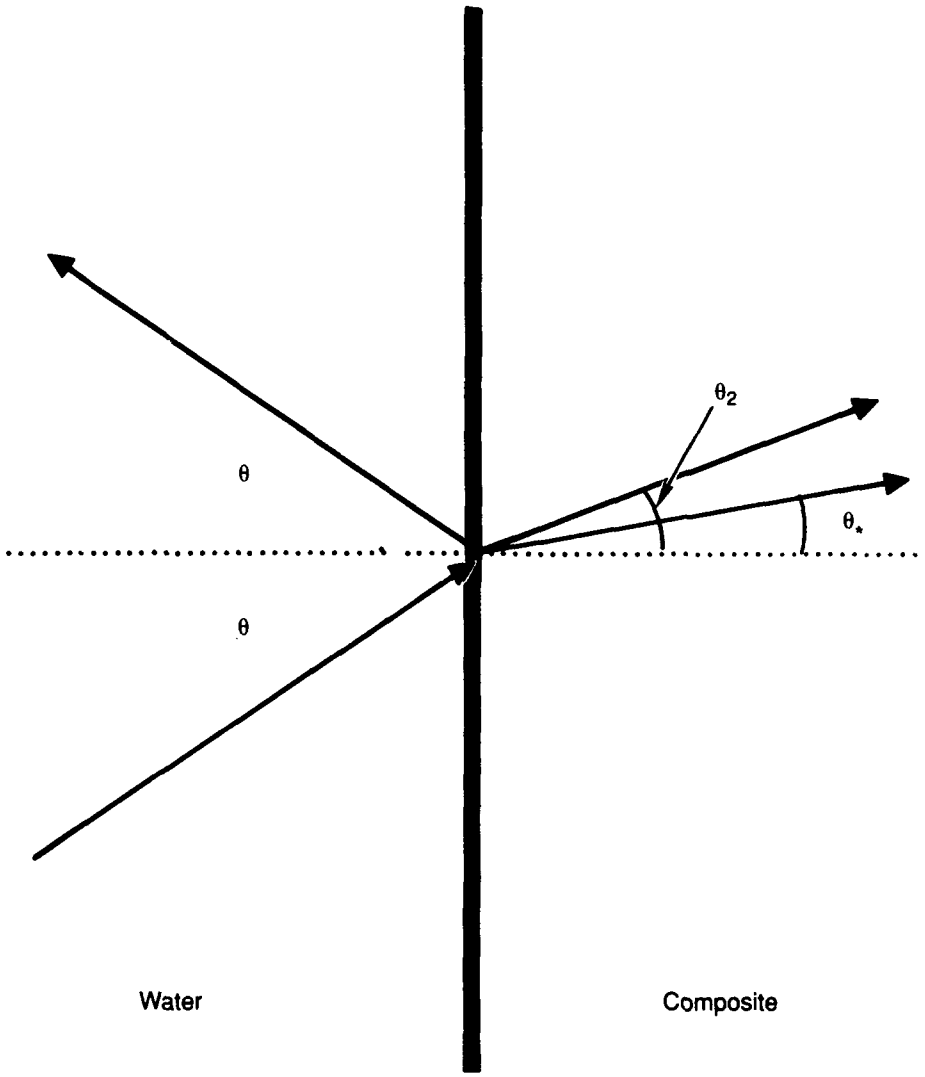

Figure 3-1. Geometry for acoustic wave reflecting from and refracting through a semi-infinite composite slab. The subscript ι (t) refers to longitudinal (transverse) waves.

The reflection and refraction of the sound wave is computed applying the boundary condition that the normal components of the stress and displacement must be continuous across the boundary and that the tangential component of the stress in the composite is zero. (See derivation in **Waves in Layered Media**, L. Brekhovskikh, Ch. 1.) The reflection coefficient can be expressed in terms of the angular-dependent acoustic impedances:

$$\begin{array}{rcll} Z_W & = & \frac{\rho_W c_W}{\cos\theta} & = \text{ acoustic impedance of the water} \\ Z_l & = & \frac{\rho_C c_l}{\cos\theta_l} & = \text{ longitudinal impedance of the composite} \\ Z_t & = & \frac{\rho_C c_t}{\cos\theta_t} & = \text{ transverse impedance of the composite,} \end{array} \qquad (3-2)$$

where $\rho_{W,C}$ is the density of water and the composite, respectively. The reflection coefficient is, then,

$$R = \frac{Z_l \cos^2\theta_t + Z_t \sin^2\theta_t - Z_W}{Z_l \cos^2 2\theta_t + Z_t \sin^2 2\theta_t + Z_W}. \qquad (3-3)$$

$|R|^2$ is the fraction of the acoustic energy that is scattered at the interface.

3.2 Conditions for Reduction of Acoustic Reflection

Suppose the goal is to design a composite that enables the reduction of reflected acoustic energy and the absorption of the transmitted energy for long wavelength incoming sound waves. The reflection coefficient should be minimized and the wavelength of the transmitted wave should shrunk to enable efficient absorption. We discuss two design approaches below.

3.2.1 Matching Z_l and Z_W

One approach for optimizing acoustic absorption is to match the longitudinal impedance of the composite to the impedance of water but reduce the wavelength of the refracted beam compared to the incidence beam. For a smooth surface, this approach works for normal incidence.

For normal incidence ($\theta = \theta_l = \theta_t = 0$), the shear waves are not excited and we obtain the same expression as for the reflection from the boundary of two liquids:

$$R = \frac{Z_l - Z_W}{Z_l + Z_W}. \qquad (3-4)$$

The reflection coefficient is minimized if the impedances are matched, $Z_l = Z_W$ or

$$\rho_W c_W = \rho_C c_l. \qquad (3-5)$$

To shrink the wavelength, which is proportional to the sound speed, we require:

$$c_l \ll c_W. \qquad (3-6)$$

Since the longitudinal sound speed can be expressed in terms of the bulk and shear moduli,

$$c^2_{long.} = \frac{3K + 4G}{3\rho},$$

the conditions in Equations (3-5) and (3-6) can be rewritten:

$$\begin{aligned} \rho_C(3K_s + 4G_s) &= \rho_W(3K_W) \\ \frac{3K_s+4G_s}{\rho_C} &\ll \frac{3K_W}{\rho_W}, \end{aligned} \qquad (3-7)$$

where the subscript s are effective values in the composite and K_W is the bulk modulus of the water.

[The conditions in Equation (3-7) are similar to conditions for reducing the reflection of electromagnetic waves by a dielectric medium. In the dielectric analogue, the impedance is the square root of the magnetic permeability, μ', divided by the dielectric constant, ϵ'. The speed of light in the medium is $c_0/\sqrt{\epsilon'\mu'}$, where c is the speed in vacuo. Hence, the analogous conditions are

$$\begin{array}{rcl} \sqrt{\mu'\epsilon'} & = & \sqrt{\mu_0\epsilon_0} \\ \sqrt{\epsilon'\mu'} & \gg & \sqrt{\epsilon_0\mu_0}, \end{array} \qquad (3-8)$$

where the subscript 0 designates values in vacuo. To satisfy the conditions for the dielectric medium, both the dielectric constant and the magnetic permeability need to be increased in the composite but their ratio needs to remain equal to their ratio in vacuo.]

As the incoming waves move away from normal incidence, shear waves are excited. From Equation (3-3), it appears at first that perfect reflection can be obtained provided both the longitudinal and shear impedances of the composite are matched to the impedance of water: $Z_t = Z_l = Z_W$. However, here one can show there is a no-go theorem. Matching the longitudinal and transverse impedances in the composite requires $c_l = c_t$. Yet, the longitudinal sound speed is $c_l = \sqrt{(3K + 4G)/3\rho}$ and the transverse sound speed is $c_t = \sqrt{G/\rho}$. Consequently, $c_l/c_t \geq \sqrt{4/3}$ for any positive K and G, and the impedance condition is necessarily violated. Therefore, the conditions in Equation (3-7) are only effective for normal incidence; away from normal incidence, the excitation of shear waves results in non-zero reflection coefficients proportional to θ^2.

The θ-dependence can be reduced by applying the composite on a "locally reactive" surface (see, for example, *Brekhovskikh*, 1960). Consider, for

example, a surface with a high density of open vertical pores whose mean size and separation are small compared to the wavelength of the incident sound wave (see Figure 3-2). In this case, the the scattering is determined by the local acoustic pressure and is not dependent on the scattering angle.

3.2.2 Matching Z_t and Z_W

In the first design, we took advantage of the fact that shear waves are not excited near normal incidence. If Z_l is matched to Z_W, longitudinal waves only are refracted; the wavelength is shrunk assuming that one can obtain a material that effectively absorbs short wavelength *longitudinal* excitations.

In this second design, the approach is to excite shear waves rather than longitudinal waves in the composite. If the angle of incidence is

$$\theta_{crit} = \sin^{-1}\left(\frac{c_W}{\sqrt{2}c_t}\right), \qquad (3-9)$$

Equation (3-1) then implies $\theta_t = \pi/4$. According to Equation (3-3), the reflection coefficient is

$$R = \frac{Z_t - Z_W}{Z_t + Z_W}. \qquad (3-10)$$

No longitudinal waves are excited and the reflection coefficient is independent of Z_l. To optimize absorption, one requires $Z_t = Z_W$ or

$$\rho_C c_t = \rho_W c_W / \sqrt{2 - (c/c_t)^2} \qquad (3-11)$$

and, to shrink the wavelength,

$$c_t \ll c_W \qquad (3-12)$$

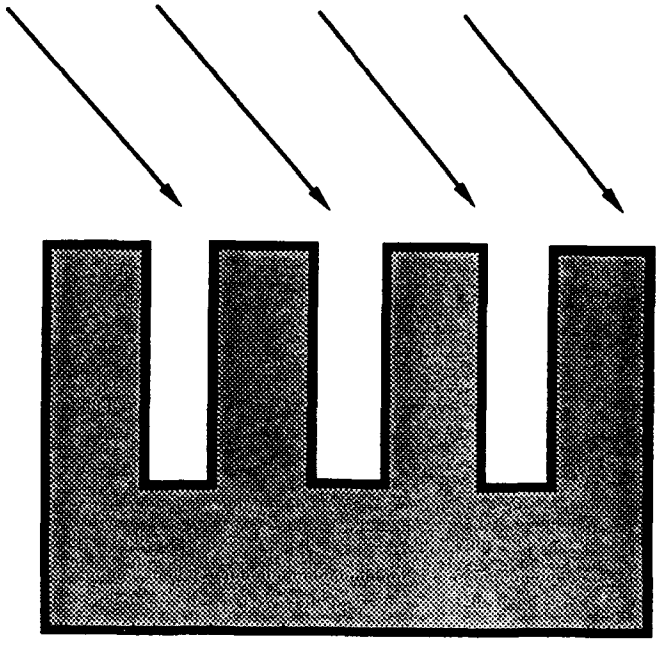

Figure 3-2. Possible geometry for a locally reactive surface that leads to θ independent scattering.

Since $c_t = \sqrt{G_*/\rho_C}$ and $c_W = \sqrt{K_W/\rho_W}$, the latter condition reduces to:

$$G_*/\rho_C \ll G_*/\rho_W \qquad (3-13)$$

For normal incidence on a surface, one can imagine coating the surface with a layer of material satisfying the above conditions and shaping the surface as shown in Figure 3-3. However, there is a fundamental limitation in the degree of wavelength shrinkage. Suppose the wavelength is to be shrunk by a factor of $\sigma > 1$: i.e., $c_W/c_t = \sigma$. From the impedance matching condition, Equation (3-11), there is the condition

$$\frac{\rho_C}{\rho_W} = \frac{\sigma}{\sqrt{2-\sigma^2}}. \qquad (3-14)$$

Consequently, the maximum wavelength shrinkage is by $\sigma = \sqrt{2}$.

The advantage of this approach is that the incident longitudinal wave is transformed into a pure shear wave in the composite, which might be easily absorbed. The disadvantage is the marginal wavelength reduction.

3.3 Effective Medium Theory and Reduction of Acoustic Reflection

Effective medium theory suggests the optimal strategy to design composite materials that reduce acoustic reflection at normal incidence, say. Consider the first (and probably preferable) design approach above. According to Equation (3-7), a material with $K_* = K_W$, $G_* \ll K_*$, and $K_*/\rho_s \ll K_W/\rho$ has acoustic impedance matched to the water but a much smaller sound

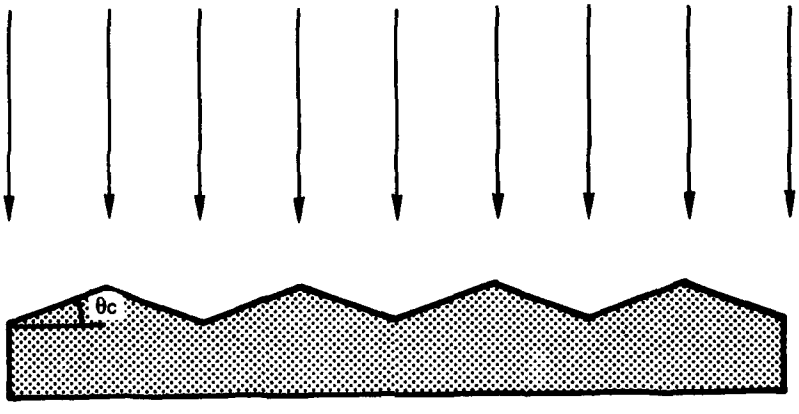

Figure 3-3. Geometry for optimal acoustic absorption for materials in which $Z_t = Z_w$.

speed. The bulk (and shear) modulus of solid materials are normally much greater than the bulk modulus of a liquid. To meet the necessary conditions, one wants to make a material that is very soft but very dense.

The effective medium theory shows that a tiny fractional volume of soft disk-like inclusions of air, say (e.g., to obtain a small bulk and shear modulus) can dramatically soften a material. In Figure 3-4, we have computed the sound speed for a material with disk-like and sphere-like inclusions of gas ($K_i \approx 0$, $G_i \approx\approx 0$, $c_i \approx 0$). Sphere-like inclusions only modestly affect the sound speed.[1] Disk-like inclusions dramatically reduce the sound speed even for relatively small fractional volumes. If a material contains cracks occupied by air, say, it will behave similar to the soft disk inclusion limit. The fact that the cracks occupy a small fractional volume means that the mean density in the composite can remain high. Consequently, the wavelength of the refracted waves can be shrunk. If the wavelength is to be shrunk by a factor σ, but the impedance is to be matched, we require $\rho_s = \rho/\sigma$. From this, we can see that the fundamental limitation is the density. Even if the cracks occupy negligible fractional volume, it is difficult to obtain a material such that $\sigma > 10$, say.

In the second design approach (Figure 3-3), it is sufficient to obtain a material with a small shear modulus only. From Equation (2-17), one observes that thin-disk inclusions of liquid (which have small shear modulus)

[1] Note that our expressions, Equations (2-4) and (2-14), predict the sound speed for the case of spherical inclusions that does not approach zero even when the fractional volume of inclusions approaches unity. This illustrates that our effective medium approximation breaks down as the inclusion volume approaches unity. Our thin-disk results apply in the limit of small inclusion volume where the theory should be valid.

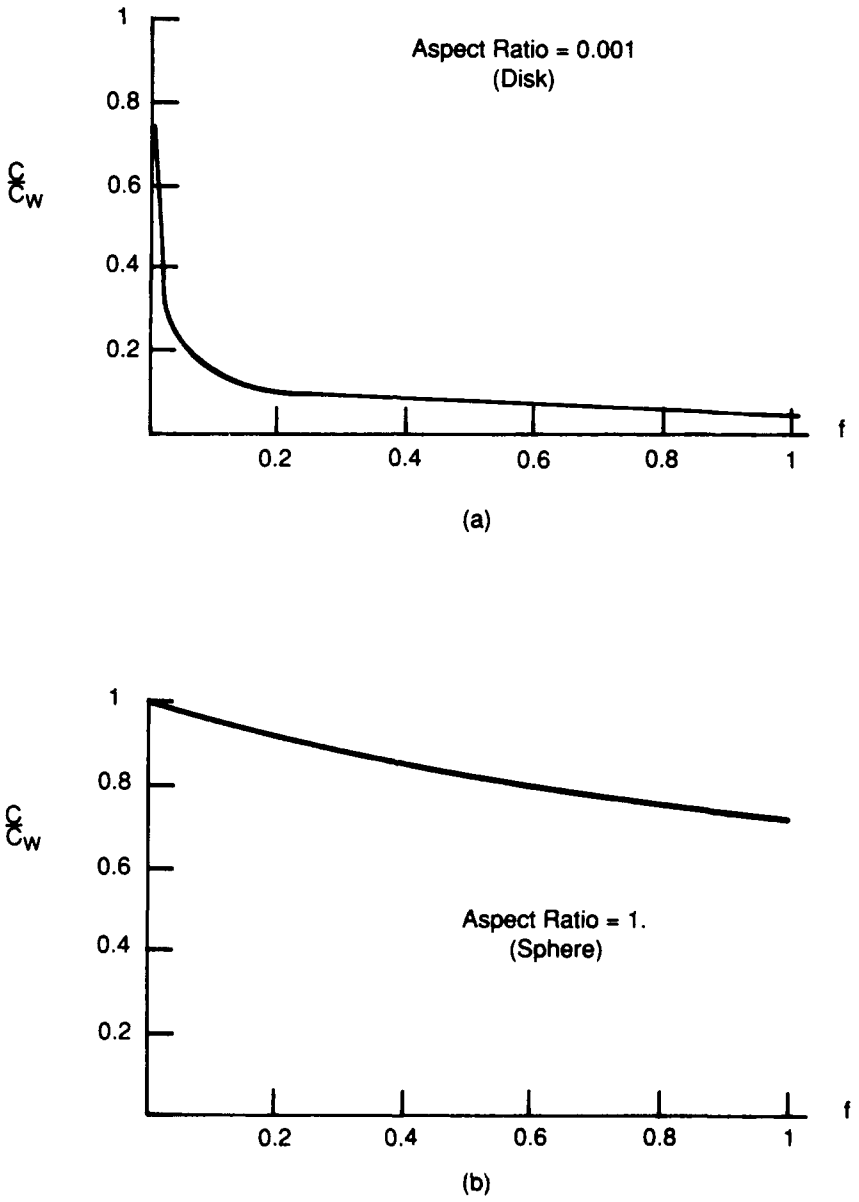

Figure 3-4. Sound speed f versus fractional inclusion volume f for disk-like and sphere-like inclusions.

is sufficient to effectively reduce the shear modulus of the composite and maintain high density. However, as shown by Equation (3-14), the maximal wavelength shrinkage is a factor of $\sqrt{2}$.

4 CONCLUSIONS

Effective medium theory can be used to determine the effect of a random distribution of impurities or inclusions on the elastic properties of an otherwise homogeneous material. The effect is characterized in terms of modified or "effective" bulk and shear moduli of the composite material.

The effective medium theory has been developed here for a spatially and orientational isotropic distribution of ellipsoidal inclusions and the effective elastic constants have been computed as a function of the concentration and aspect ratio of the inclusions. The theory is valid in the limit of small fractional volume of inclusions. The basic conclusions are:

- Thin-disk or crack-like inclusions are the most effective means of softening (or hardening) a composite material. Even a small fractional volume of air inclusions dramatically suppresses the bulk and shear moduli as the width of the disks becomes small.
- The effect of needle-like inclusions is comparable to that of sphere-like inclusions. In either case, significant hardening or softening of the composite occurs only if the inclusions occupy a substantial fractional volume.
- Composites with thin-disk inclusions of air may be effective materials for acoustic absorption. The composite can be impedance matched to an external liquid medium (water, say) such that refracted waves have

reduced wavelength. The wavelength reduction is by a factor equal to the ratio of the composite density to water density, which is a significant limitation.

- In the discussion of acoustic absorption, semi-infinite slabs consisting of macroscopically homogeneous composites have been considered. In practice, multi-layered coatings can be applied with elastic behavior that varies from layer to layer. Here, too, effective medium theory can be a useful guide. However, our approximation is only valid when the slab thickness is much greater than the acoustic wavelength.

- We note that this analysis has focussed only on impedance matching and wavelength shrinkage, but does not directly address materials design for effective attenuation. Since the maximal wavelength shrinkage was shown to be by only a factor of 10 or so, effective attenuation is very difficult to achieve in thin coatings. By comparison, electromagnetic wavelenth can be shrunk by many orders of magnitude so that thin, absorptive coatings for electromagnetic waves are more feasible.

REFERENCES

1. Berryman, J. G., *J. Acoust. Soc. Am.* 68(6), 1809, 1820 (1980).

2. Brekhovskikh, L. M., **Waves in Layered Media**, (Academic Press, New York, 1960) Ch. 1.

3. The Dielectric Properties of Composites (U), by David Nelson, JASON Report No. JSR-88-100, SECRET (MITRE Corporation, McLean, VA, 1990)

4. Einstein, A., *Ann. Phys.* 19, 289 (1906); and 34, 591 (1911).

5. Eshelby, J.D., *Proc. R. Soc. London Ser. A* 241, 376 (1957).

6. Hashin, Z. and Shtrikman, S., *J. Mech. Phys. Solids* 10, 335 (1962); and 11, 140 (1963).

7. Hill, R., *J. Mech. Phys. Solids* 11, 372 (1963).

8. Korringa, J., Brown, R.J.S., Thompson, D.D., and Runge, R.J., *J. Geophys. Res.* 84 (B10), 5591 (1979).

9. Landau, L.M., and Lifshitz, E. M., **Fluid Mechanics**, (Pergamon Press, Oxford, 1959) pp. 248-9.

10. Maxwell-Garnett, J.C., *Phil. Trans. R. Soc.* 203, 385 (1904).

11. Watt, J.P., Davies, G.F. and O'Connell, R.J., *Rev. Geophys. Space Phys.* 14(4), 541 (1976).

12. Wu, T.T., *Int. J. Solids Struct.* 2, 1 (1966).

13. Zeller, R. and Dederichs, P.H., *Phys. Status Solid.* B55(2), 831 (1973).

DISTRIBUTION LIST

CMDR & Program Executive Officer
US Army/CSSD-ZA
Strategic Defense Command
PO Box 15280
Arlington, VA 22215-0150

Mr John M Bachkosky
Deputy DDR&E
The Pentagon
Room 3E114
Washington, DC 20301

Dr Joseph Ball
Central Intelligence Agency
Washington, DC 20505

Dr Arthur E Bisson
DASWD (OASN/RD&A)
The Pentagon
Room 5C675
Washington, DC 20350-1000

Dr Albert Brandenstein
Chief Scientist
Office of Natl Drug Control Policy
Executive Office of the President
Washington, DC 20500

Mr Edward Brown
Assistant Director
Nuclear Monitoring Research Office
DARPA
3701 North Fairfax Drive
Arlington, VA 22203

Dr Herbert L Buchanan III
Director
DARPA/DSO
3701 North Fairfax Drive
Arlington, VA 22203

Dr Curtis G Callan Jr
Physics Department
PO Box 708
Princeton University
Princeton, NJ 08544

Dr Ferdinand N Cirillo Jr
Central Intelligence Agency
Washington, DC 20505

Brig Gen Stephen P Condon
Deputy Assistant Secretary
Management Policy &
Program Integration
The Pentagon Room 4E969
Washington, DC 20330-1000

Ambassador Henry F Cooper
Director/SDIO-D
Room 1E1081
The Pentagon
Washington, DC 20301-7100

DARPA Library
3701 North Fairfax Drive
Arlington, VA 22209-2308

DISTRIBUTION LIST

Mr John Darrah
Senior Scientist and Technical Advisor
HQAF SPACOM/CN
Peterson AFB, CO 80914-5001

Dr Gary L Denman
Acting Director
DARPA/DIRO
3701 North Fairfax Drive
Arlington, VA 22203-1714

Col Doc Dougherty
DARPA/DIRO
3701 North Fairfax Drive
Arlington, VA 22203

DTIC [2]
Defense Technical Information Center
Cameron Station
Alexandria, VA 22314

Mr John N Entzminger
Chief, Advance Technology
DARPA/ASTO
3701 North Fairfax Drive
Arlington, VA 22203

CAPT Kirk Evans
Director Undersea Warfare
Space & Naval Warfare Sys Cmd
Code PD-80
Department of the Navy
Washington, DC 20363-5100

Mr F Don Freeburn
US Department of Energy
Code ER-33
Mail Stop G-236
Washington, DC 20585

Dr S William Gouse
Sr Vice President and General Manager
The MITRE Corporation
Mail Stop Z605
7525 Colshire Drive
McLean, VA 22102

Mr Thomas H Handel
Office of Naval Intelligence
The Pentagon
Room 5D660
Washington, DC 20350-2000

Maj Gen Donald G Hard
Director of Space and SDI Programs
Code SAF/AQS
The Pentagon
Washington, DC 20330-1000

Dr Robert G Henderson
Director
JASON Program Office
The MITRE Corporation
7525 Colshire Drive Z561
McLean, VA 22102

Dr Barry Horowitz
President and Chief Executive Officer
The MITRE Corporation
202 Burlington Road
Bedford, MA 01730-1420

DISTRIBUTION LIST

Dr William E Howard III [2]
Director For Space
and Strategic Technology
Office/Assistant Secretary of the Army
The Pentagon Room 3E474
Washington, DC 20310-0103

Dr Gerald J Iafrate
US Army Research Office
PO Box 12211
4300 South Miami Boulevard
Research Triangle Park, NC 27709-2211

JASON Library [5]
The MITRE Corporation
Mail Stop W002
7525 Colshire Drive
McLean, VA 22102

Dr George Jordy [25]
Director for Program Analysis
US Department of Energy
MS ER30 Germantown
OER
Washington, DC 20585

Dr O'Dean P Judd
Los Alamos National Lab
Mail Stop A-110
Los Alamos, NM 87545

Mr Robert Madden [2]
Department of Defense
National Security Agency
Attn R-9 (Mr Madden)
Ft George G Meade, MD 20755-6000

Dr Arthur F Manfredi Jr [10]
OSWR
Central Intelligence Agency
Washington, DC 20505

Mr Joe Martin
Director
OUSD(A)/TWP/NW&M
Room 3D1048
The Pentagon
Washington, DC 20301

Mr Ronald Murphy
DARPA/ASTO
3701 North Fairfax Drive
Arlington, VA 22203-1714

Dr Julian C Nall
Institute for Defense Analyses
1801 North Beauregard Street
Alexandria, VA 22311

Dr Gordon C Oehler
Central Intelligence Agency
Washington, DC 20505

Dr Peter G Pappas
Chief Scientist
US Army Strategic Defense Command
PO Box 15280
Arlington, VA 22215-0280

DISTRIBUTION LIST

Dr Bruce Pierce
USD(A)/D S
Room 3D136
The Pentagon
Washington, DC 20301-3090

Mr John Rausch [2]
Division Head 06 Department
NAVOPINTCEN
4301 Suitland Road
Washington, DC 20390

Records Resources
The MITRE Corporation
Mailstop W115
7525 Colshire Drive
McLean, VA 22102

Dr Fred E Saalfeld
Director
Office of Naval Research
800 North Quincy Street
Arlington, VA 22217-5000

Dr John Schuster
Technical Director of Submarine
and SSBN Security Program
Department of the Navy OP-02T
The Pentagon Room 4D534
Washington, DC 20350-2000

Dr Barbara Seiders
Chief of Research
Office of Chief Science Advisor
Arms Control & Disarmament Agency
320 21st Street NW
Washington, DC 20451

Dr Philip A Selwyn [2]
Director
Office of Naval Technology
Room 907
800 North Quincy Street
Arlington, VA 22217-5000

Dr Paul Joseph Steinhardt
David Rittenhouse Laboratory
Department of Physics
33rd & Walnut Streets
University of Pennsylvania
Philadelphia, PA 19104-6396

Superintendent
CODE 1424
Attn Documents Librarian
Naval Postgraduate School
Monterey, CA 93943

Dr George W Ullrich [3]
Deputy Director
Defense Nuclear Agency
6801 Telegraph Road
Alexandria, VA 22310

Ms Michelle Van Cleave
Asst Dir/National Security Affairs
Office/Science and Technology Policy
New Executive Office Building
17th and Pennsylvania Avenue
Washington, DC 20506

Mr Richard Vitali
Director of Corporate Laboratory
US Army Laboratory Command
2800 Powder Mill Road
Adelphi, MD 20783-1145

DISTRIBUTION LIST

Dr Edward C Whitman
Dep Assistant Secretary of the Navy
C3I Electronic Warfare & Space
Department of the Navy
The Pentagon 4D745
Washington, DC 20350-5000

Mr Donald J. Yockey
U/Secretary of Defense
For Acquisition
The Pentagon Room 3E933
Washington, DC 20301-3000

Dr Linda Zall
Central Intelligence Agency
Washington, DC 20505

Mr Charles A Zraket
Trustee
The MITRE Corporation
Mail Stop A130
202 Burlington Road
Bedford, MA 01730